The evolution of disc galaxies

Shaun M. Cole, Carlton Baugh, Carlos Frenk, Cedric Lacey and Andrew Benson

Phil. Trans. R. Soc. Lond. A 2000 **358**, 2093-2107
doi: 10.1098/rsta.2000.0632

10.1098/rsta.2000.0632

The evolution of disc galaxies

By Shaun M. Cole[1], Carlton Baugh[1], Carlos Frenk[1], Cedric Lacey[2] and Andrew Benson[1]

[1] *Department of Physics, University of Durham, South Road, Durham DH1 3LE, UK*
[2] *SISSA, via Beirut, 2-4, 34014 Trieste, Italy*

We briefly describe the physical processes that are included in our semi-analytic model of hierarchical galaxy formation. We review some of the low redshift properties of one such model constructed assuming a ΛCDM cosmology. We examine the evolutionary paths of typical bright disc galaxies in this model. This case study serves to illustrate the generic features of galaxy evolution in hierarchical models. It is demonstrated that the richness of galaxy evolution in this model is hidden when one looks at the evolution of global properties such as the galaxy luminosity function. We also quantify a generic prediction of hierarchical galaxy formation, namely that galaxies were physically smaller in the past. This model is consistent with recent high redshift observations and the reported evolution of galaxy sizes lends general support to hierarchical galaxy formation.

Keywords: galaxies; formation; evolution

1. Introduction

Observations now probe the properties of galaxy populations over a large fraction of the age of the Universe (e.g. Steidel *et al.* 1996; Ellis *et al.* 1996; Lilly *et al.* 1996; Adelberger *et al.* 1998). Furthermore, we can look forward to a much more detailed study of the high redshift Universe with the many instruments soon to be commissioned on the growing generation of new 8 m class telescopes. Over the lookback time probed by these observations the conventional cold-dark-matter-dominated models of structure formation predict very strong evolution of the distribution of dark matter. Thus the process of galaxy formation will be greatly influenced and probably largely determined by the dynamical evolution of the dark matter.

Here we use the powerful technique of semi-analytic galaxy formation to investigate galaxy evolution within the framework set by the hierarchical merging of dark matter halos. A simpler but useful treatment of disc galaxy formation within the same framework, but ignoring the detailed merger histories of the galaxies, is given by Mo *et al.* (1998) and Mao *et al.* (1998). An even simpler model for the disc evolution is given by Dalcanton *et al.* (1997). In § 2, we briefly describe the physical processes that are included in the Cole *et al.* (2000) semi-analytic model of hierarchical galaxy formation. In § 3, we specify a completely determined ΛCDM model and compare its redshift zero properties with observations, a subset of which have been used to constrain the parameters of the model. This model is used as a case study to illustrate some of the generic features of hierarchical galaxy formation. In § 4, we examine the evolutionary properties of this model and examine in detail the formation of several randomly selected bright disc galaxies. We conclude in § 5.

2. The model

A full description of the current Durham semi-analytic galaxy formation model, complete with an exploration of how the predictions depend on parameter variations and how they compare with observational data, can be found in Cole *et al*. (2000). Here we simply describe the main features of the model.

(*a*) *Merger trees*

We use a simple new Monte Carlo algorithm to generate merger trees that describe the formation paths of randomly selected dark matter halos. Our algorithm is based directly on the analytic expression for halo merger rates derived by Lacey & Cole (1993). The algorithm enables the merger process to be followed with high time resolution, as time-steps are not imposed on the tree but rather are controlled directly by the frequency of mergers.

(*b*) *Halo structure and gas cooling*

We assume that the dark matter in virialized halos is well described by the NFW density profile (Navarro *et al*. 1997). We further assume that any diffuse gas present during a halo merger is shock heated to the virial temperature of the halo. The density profile we adopt for the hot gas is less centrally concentrated than that of the dark matter and is chosen to be in agreement with the results of high resolution simulations of non-radiative gas (e.g. Frenk *et al*. 1999). We estimate the fraction of gas that can cool in a halo by computing the radius at which the radiative cooling time of the gas equals the age of the halo. The gas that cools is assumed to conserve angular momentum and settle into a rotationally supported disc. Thus, the initial angular momentum of the halo, which we assign using the well-characterized distribution of spin parameters found for halos in N-body simulations, determines the size of the resulting galaxy disc. In computing the size of the disc we also take account of the contraction of the inner part of the halo caused by the gravity of the disc.

In direct hydrodynamic simulations of galaxy formation (Navarro *et al*. 1995; Navarro & Steinmetz 1999), the assumption that angular momentum is conserved during the assembly of a galaxy disc is broken. In these simulations, galaxies are assembled by the merging of cold lumps, which are effective at transferring angular momentum to their common dark matter halo prior to merging. The resulting disc galaxies have smaller scale-lengths and lower specific angular momenta than observed galaxy discs. As we shall see below, if instead angular momentum conservation is assumed, the resulting disc scale-lengths match those observed quite well. Thus, it seems likely that some process not currently included in the direct simulations must be responsible for preventing efficient angular momentum transport. The obvious candidate is stellar feedback which could suppress the formation of cold sub-galactic lumps prior to the assembly of the final disc and so reduce angular momentum transport. This is an important problem which merits further attention.

(*c*) *Star formation and feedback*

The processes of star formation and stellar feedback are the most uncertain to model. We adopt a flexible approach in which the star formation rate in the disc of cold gas is given by $\dot{M}_\star = M_{\rm cold}/\tau_\star$, with the time-scale $\tau_\star$ parametrized as

$$\tau_\star = \epsilon_\star^{-1}\tau_{\rm disc}(V_{\rm disc}/200\ {\rm km\ s^{-1}})^{\alpha_\star}. \tag{2.1}$$

We also adopt a feedback model in which for every solar mass of stars formed,

$$\beta = (V_{\rm disc}/V_{\rm hot})^{-\alpha_{\rm hot}} \tag{2.2}$$

solar masses are assumed to be reheated and ejected from the disc as a result of energy input from young stars and supernovae. In these formulae, $\tau_{\rm disc}$ and $V_{\rm disc}$ are the dynamical time and circular velocity of the disc; $\epsilon_\star$, $\alpha_\star$, $\alpha_{\rm hot}$ and $V_{\rm hot}$ are the model parameters. These parameters must be fixed by reference to observations of galaxy properties in the local Universe.

(*d*) *Galaxy mergers*

Mergers between galaxies can occur, subsequent to the merger of their dark matter halos, if dynamical friction causes the orbits of the galaxies to decay. The result of a merger depends on the mass ratio of the merging galaxies. If they are comparable, $M_{\rm smaller} > f_{\rm ellip}M_{\rm larger}$, then the merger is said to be violent and results in the formation of a spheroid. At this point, any cold gas present in the merger is assumed to undergo a burst of star formation, with a time-scale equal to the dynamical time of the forming spheroid and with feedback estimated using equation (2.2), but with the circular velocity of the spheroid replacing that of the disc. The size of the resulting spheroid is estimated assuming energy conservation in the merger (once dynamical friction has eroded the orbits to the point where the galaxies interpenetrate) and the virial theorem. For minor mergers, $M_{\rm smaller} < f_{\rm ellip}M_{\rm larger}$, we simply assume the cold gas is accreted by the disc and the stars by the bulge of the larger galaxy. Taking $f_{\rm ellip} = 0.3$ gives a relative frequency off ellipticals, S0s and spirals roughly in accord with local observations.

(*e*) *Stellar population synthesis and dust*

To convert the calculated star formation histories of each galaxy into observable luminosities and colours we use the stellar population synthesis model of Bruzual & Charlot (1993, 2000) together with the three-dimensional dust model of Ferrara *et al.* (1999). For the former, we adopt the initial mass function of the solar neighbourhood as parametrized by Kennicutt (1983) and for the latter we adopt their Milky Way extinction law and assume that the dust-to-gas ratio in the cold gas disc scales with metallicity.

3. Redshift zero properties

The response of this galaxy formation model to parameter changes has been explored extensively in Cole *et al.* (2000). They also present a reference model for a ΛCDM cosmology (with $\Omega_0 = 0.3$, $\Lambda_0 = 0.7$ and $h = 0.7$), which reproduces many of the low redshift properties of the observed galaxy distribution. To illustrate the behaviour

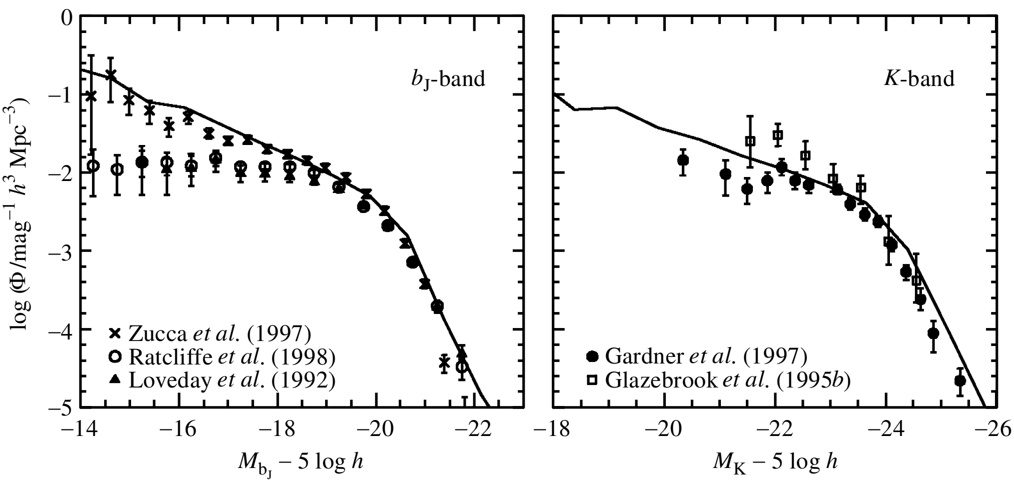

Figure 1. The b_J and K-band luminosity functions of our ΛCDM model compared with a variety of observational estimates (symbols).

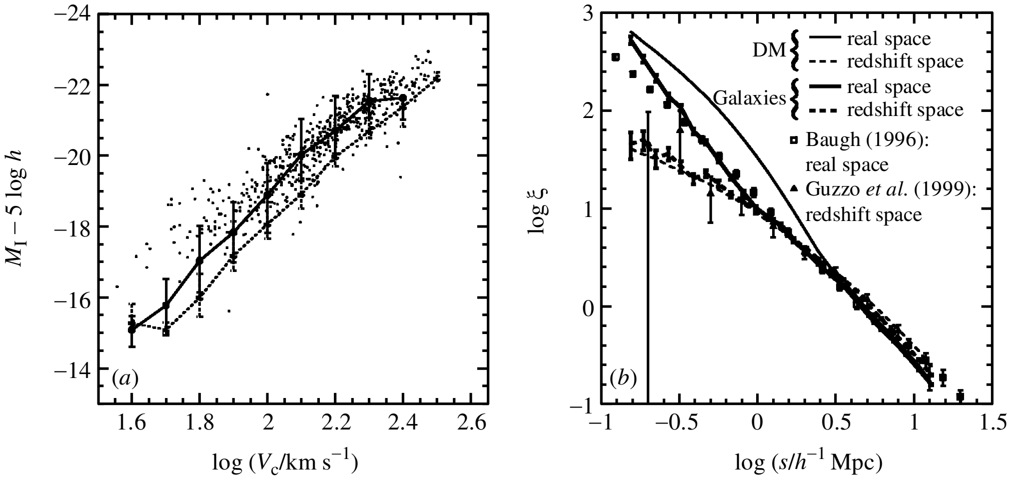

Figure 2. (a) This shows the I-band Tully–Fisher relation. The points are the observational data of Mathewson *et al*. (1992). The solid line and error bars indicate the median and scatter in the model. Here the circular velocity that is plotted is that at the virial radius of the halo in which the galaxy formed. If instead one plots the circular velocity at half mass radius of the galaxy disc, the relation shifts to that indicated by the dashed line. (b) This shows real/redshift space correlation functions of the dark matter (thin solid/dashed) and galaxies (thick solid/dashed) and also observational estimates of the real and redshift space galaxy correlation functions.

of hierarchical galaxy formation models we have chosen to explore the properties of this fully specified ΛCDM model.

In figures 1 and 2 we show a variety of the $z = 0$ properties of this model and compare them with observational data. The luminosity functions (figure 1) have been used to constrain most of the galaxy formation model parameters. Additional parameters have been set by reference to slope of the Tully–Fisher relation (figure 2a). The slope and scatter of this relation are reproduced well, but the model disc circular

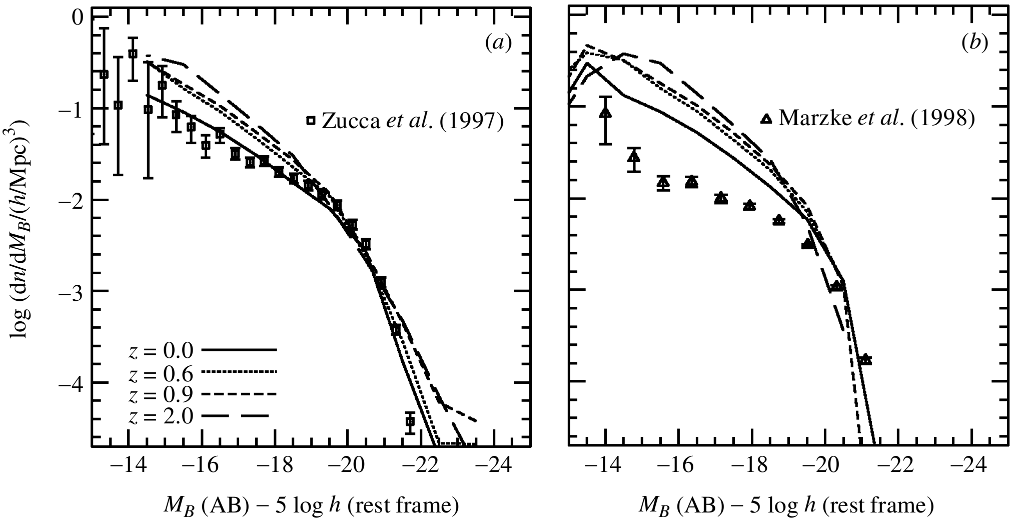

Figure 3. The evolution of the B-band luminosity function, (a) for all galaxies and (b) for disc-dominated galaxies only. The data points show corresponding observational estimates at $z = 0$.

velocities are *ca.* 30% too large. (If one instead plots the circular velocities at the virial radii of the halos in which the galaxies formed, these are typically 30% lower and result in a good match to the observed Tully–Fisher relation.) This problem with the model seems to be related to the high central densities of DM halos produced in cosmological CDM N-body simulations, as discussed recently by Navarro & Steinmetz (2000) and Steinmetz & Navarro (1999).

The real and redshift space galaxy correlation functions shown in figure 2b were not used to set model parameters, and so may be regarded as model predictions. They are in good agreement with observations. These clustering properties of the galaxy formation model were computed by combining the semi-analytic model with cosmological N-body simulations, as described in Benson *et al.* (2000a). This paper tests the robustness of these predictions to parameter variations and also explains physically why on small scales a complex scale-dependent bias arises between the clustering of the galaxies and the dark matter. The dependence of galaxy clustering in real and redshift space on galaxy properties (e.g. luminosity, morphology and colour) is calculated and compared with observational data in Benson *et al.* (2000b; see also Kauffmann *et al.* 1999a,b; Diaferio *et al.* 1999).

4. Evolution

(a) *Luminosity functions*

Figure 3 shows the prediction of our model for the evolution of the rest-frame B-band luminosity function both for the whole galaxy population and for a subsample of disc-dominated galaxies. We see that in both cases there is very little evolution of the number density of $L_\star$ galaxies out to at least redshift $z = 1$. This mild evolution, which is similar to that seen observational samples (e.g. Brinchmann 1999), could be interpreted as indicating that disc galaxies were largely in place at redshift $z = 1$ and

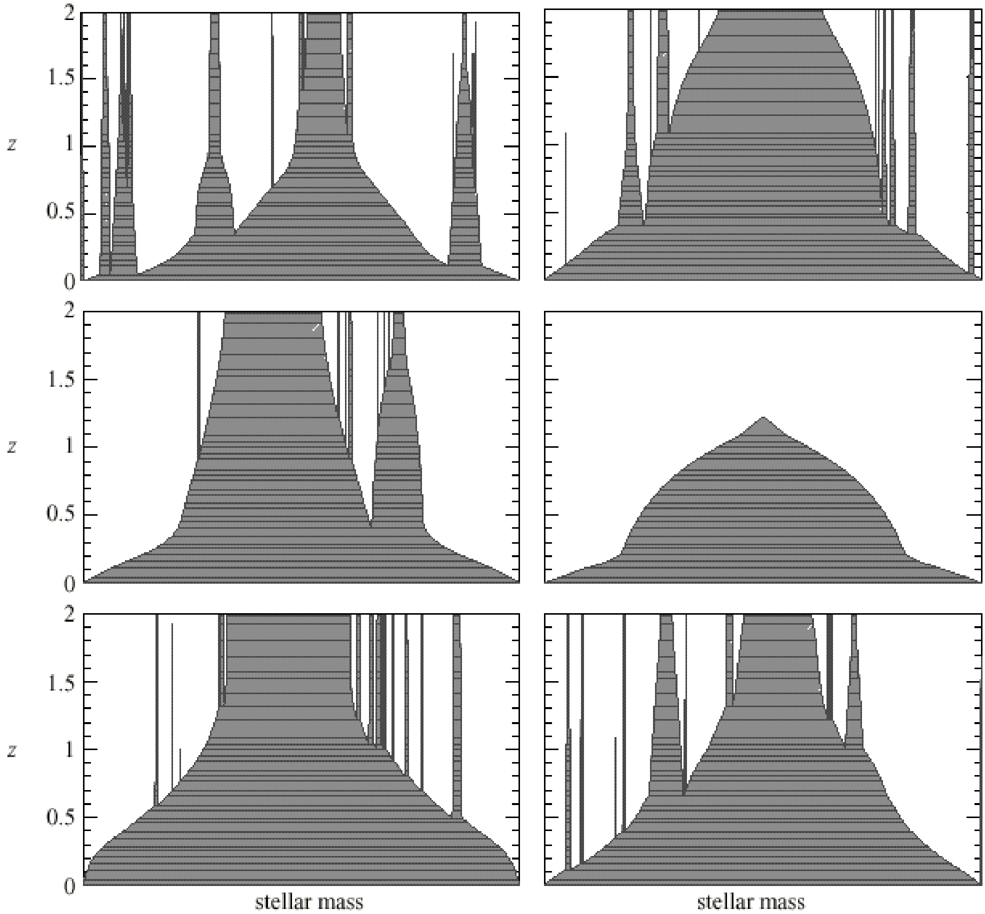

Figure 4. The formation histories of a random selection of present-day, bright, disc-dominated galaxies. At a given redshift the number of shaded components equals the number of progenitors and their widths indicate their stellar masses.

have simply gradually converted gas to stars over this time-span, at a fairly constant star formation rate. As we shall see in the next section this interpretation is in stark contrast with the actual evolution that occurs in this model.

(*b*) *Individual galaxies*

Figure 4 depicts the formation histories of a random sample of present-day, bright ($L > L_\star$), disc-dominated galaxies. (Here and below we use the term disc-dominated to denote galaxies with B-band bulge-to-total light ratios less than 0.4.) We can see that the formation histories are very varied and involve a number of mergers with progenitors of a wide range of stellar masses.

Some properties of this variety of formation paths are quantified in figure 5. Figure 5*a* shows the ratio of stellar disc mass today to that of the most massive disc progenitor at redshift $z = 1$ as a function of the present-day disc luminosity. The corresponding change in the rest-frame B-band magnitude of the disc is shown in

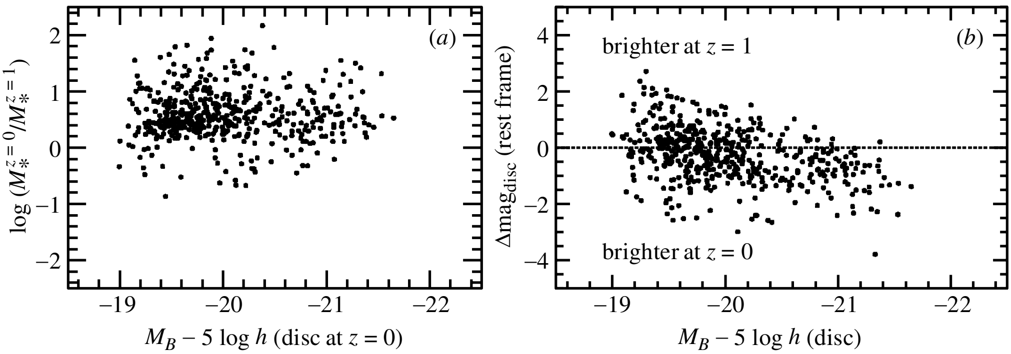

Figure 5. (a) The ratio of stellar disc mass today to that of the most-massive progenitor at redshift $z = 1$ as a function of the B-band magnitude of the present-day disc. (b) The corresponding change in B-band magnitude of the stellar disc.

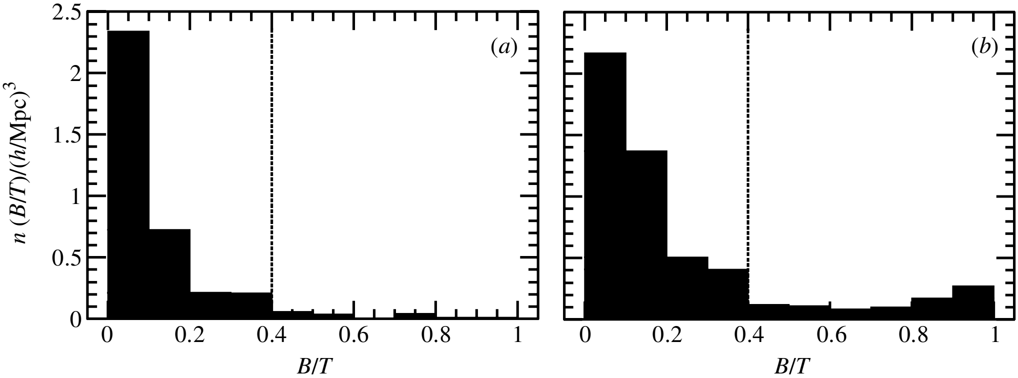

Figure 6. Distributions of B-band bulge-to-total light ratios. (a) This is the distribution at $z = 1$ for the largest progenitors of present-day bright, disc-dominated ($B/T < 0.4$) galaxies. (b) This is the distribution at $z = 0$ of the descendants of bright disc-dominated galaxies selected at $z = 1$.

figure 5b. The mean disc mass has increased by a factor of 2 to 3 over this time-span and this is accompanied by a modest increase in B-band luminosity of 0.0–0.5 mag. However, the scatter about these mean trends is large, with many discs growing by more than factor 10 in mass and disc brightnesses varying by up to ± 2 mag. The occurrence of some galaxies whose disc stellar mass decreases from redshift $z = 1$ to $z = 0$ is a result of some discs being destroyed in major mergers and later being renewed by the subsequent accretion of cooling gas.

The luminosity changes quantified above are large compared with the modest change in the characteristic luminosity, $L_\star$, during this same time-interval shown in figure 3. This implies that there can be no simple one-to-one correspondence between the brightest galaxies at redshift $z = 1$ and those today. One example of this is illustrated in figure 6, which depicts the distribution of B-band bulge-to-total luminosity ratios for bright, disc-dominated galaxies selected at (a) $z = 0$ and (b) $z = 1$. From this we see that even the morphological classification of these galaxies

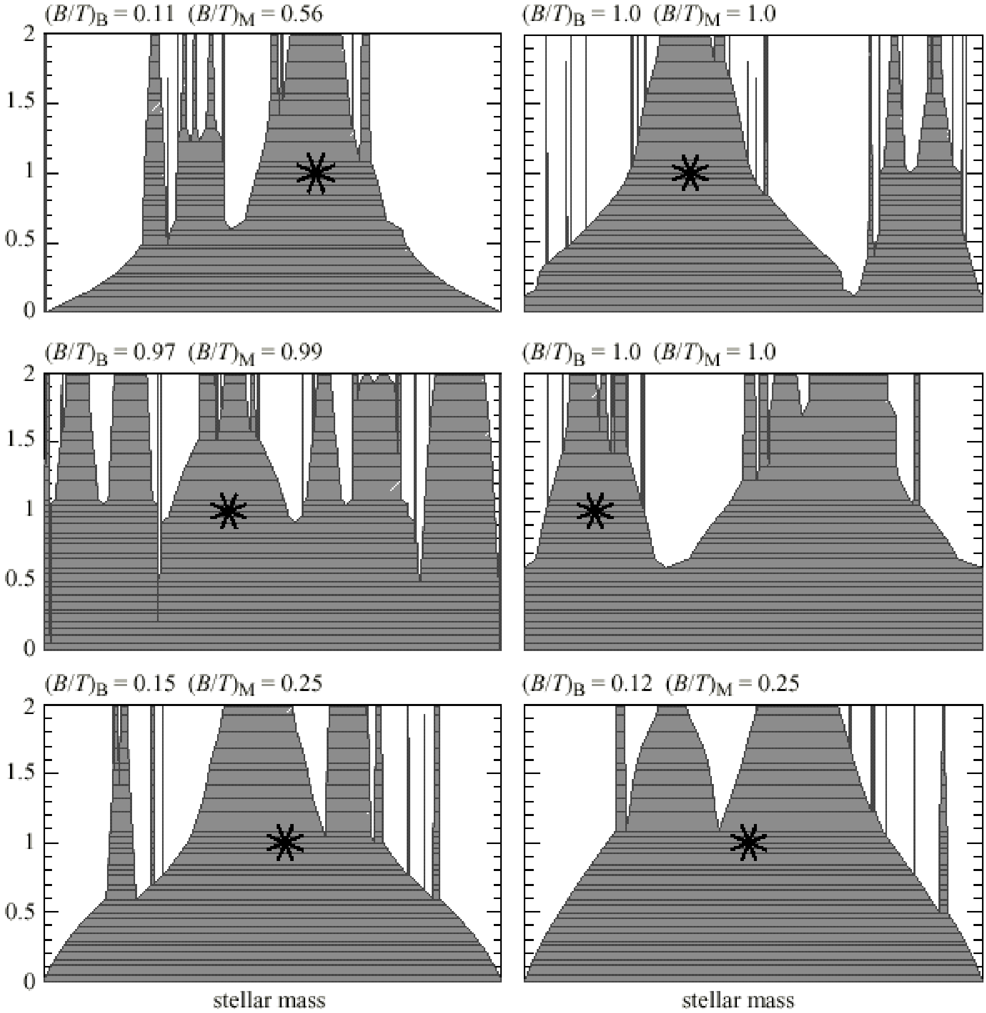

Figure 7. As figure 4, but for progenitors (indicated by the asterisks) that are selected to be bright disc-dominated galaxies at redshift $z = 1$. The bulge-to-total ratios of the descendant at $z = 0$, both by B-band light and mass, are indicated above each panel.

can vary significantly between the two epochs. In particular, a significant fraction of the bright disc galaxies at redshift $z = 1$ are destined to become elliptical galaxies at the present day.

Given these gross changes it is clear that the merger and star formation histories depicted in figure 5, while being typical for disc galaxies selected at redshift $z = 0$, will not be representative of the fate of disc galaxies selected at an earlier time. This is illustrated in figure 7, which shows the star formation and merger histories of a random sample of $z = 1$, bright ($L > L_\star$) disc-dominated galaxies. Many of the bright disc galaxies at redshift $z = 1$ are destined to undergo quite strong mergers before the present.

Figure 8 is analogous to figure 6, but for galaxies selected to be bright disc galaxies at redshift $z = 1$ rather than at $z = 0$. Here, we use different symbols to indicate the

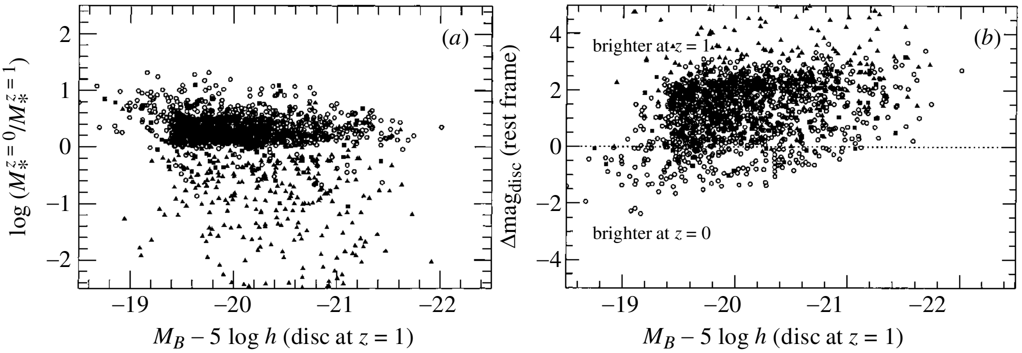

Figure 8. The change in mass and magnitude between redshifts $z = 1$ and $z = 0$ of the discs of galaxies selected as bright and disc-dominated at $z = 1$. (*a*) The ratio of stellar disc masses as a function of the B-band magnitude of the $z = 1$ disc. (*b*) The corresponding change in B-band magnitude of the stellar disc. In each panel open circles are for galaxies whose descendants at $z = 0$ are spirals (disc-dominated) and filled triangles for galaxies whose descendants are E/S0 galaxies.

morphology of the galaxy at redshift $z = 0$. Figure 8*a* shows the ratio of the stellar disc mass of the descendant at $z = 0$ to that of the largest progenitor disc at redshift $z = 1$. The corresponding change in the rest-frame B-band magnitude of the disc is shown in figure 8*b*. As in figure 6*a* we see that the mean disc mass has increased by a factor of 2 to 3 over this time-span, but now there is an additional population of discs whose masses have decreased dramatically due to mergers that result in bulge-dominated galaxies at the present day. In figure 8*b* we see that the typical disc luminosity of this sample is 1–1.5 mag brighter at $z = 1$ than at $z = 0$. The sign of this evolution is opposite to that for the sample selected at redshift $z = 0$. This can be understood in terms of the varied and non-monotonic evolution of the individual galaxy luminosities together with the fact that we have selected the brightest objects at one or other epoch. Thus, the galaxies will tend to be brightest at the epoch at which they are selected.

MATHEMATICAL, PHYSICAL & ENGINEERING SCIENCES
THE ROYAL SOCIETY A
PHILOSOPHICAL TRANSACTIONS OF

5. Observational tests

(*a*) *Deep counts*

In the previous section we have seen that in a hierarchical model, galaxy evolution is a complex process involving mergers and morphological transformations of galaxies, as well as non-monotonic evolution of their luminosities. In figure 9 we show that despite this complexity, its predictions are in good agreement with the evolution of the observed galaxy population when quantified in terms of morphologically classified galaxy counts. This figure is similar to that in Baugh *et al.* (1996), but the model curves are for the newer ΛCDM model of Cole *et al.* (2000). It is noteworthy that this hierarchical model naturally reproduces both the total observed counts and the trend for the Irregular/Merger class to become an increasing fraction of the total at fainter magnitudes.

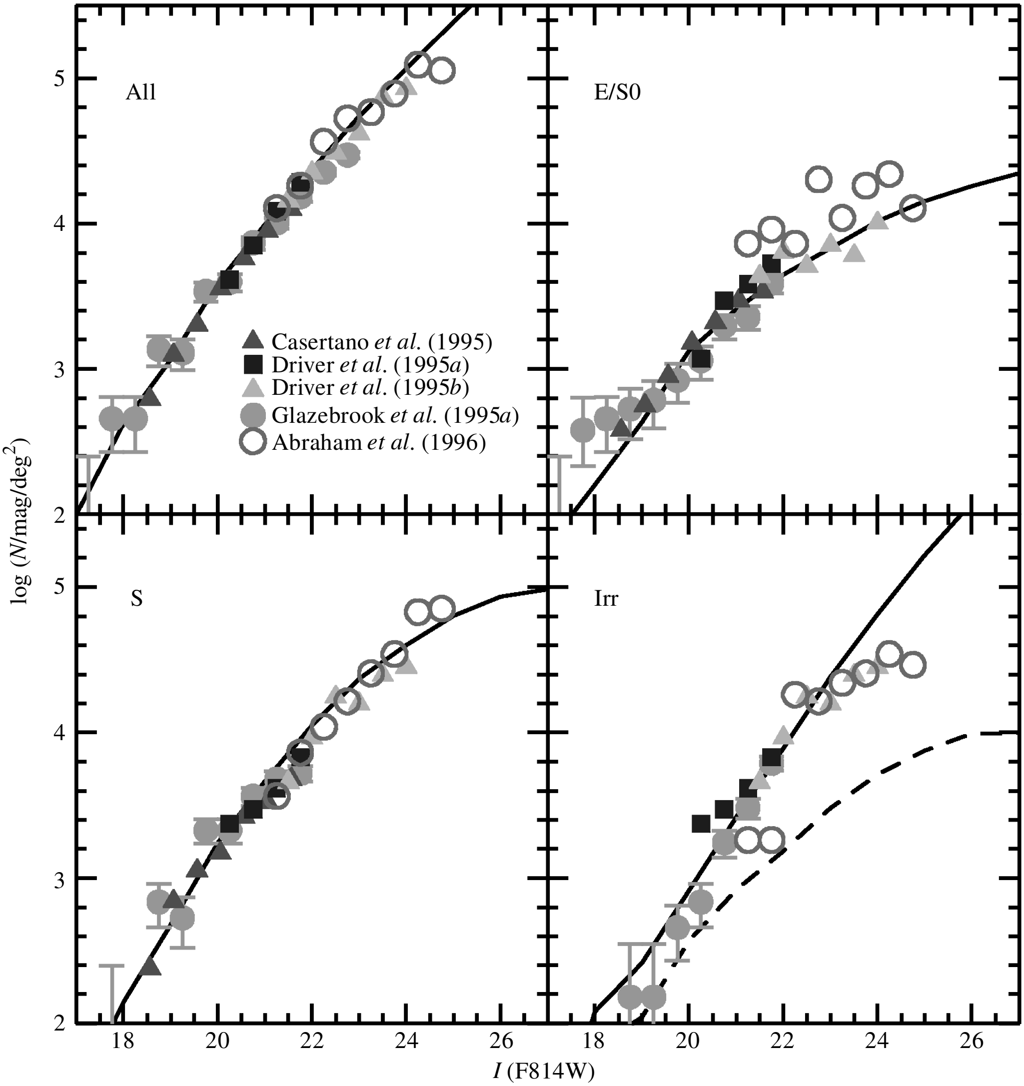

Figure 9. The total and morphologically split I-band counts compared with various observational estimates (symbols). In the model, spirals are defined (in the I-band) to have $0.05 < B/T < 0.4$, E/S0 have $B/T > 0.4$ and Irregular/Peculiars have either $B/T < 0.05$ or have experienced a merger induced burst of star formation the last 1 Gyr. The contribution of this last category to the counts is shown by the dashed curve in the final panel.

(*b*) *The stellar mass function*

In the model the relation between mass and luminosity is complicated and time-varying. Thus, much of the ambiguity in the nature of the galaxy evolution could be removed if one could study the stellar mass rather than the luminosity. This is becoming possible using deep redshift surveys with infrared colours so that evolutionary and k-corrections can be estimated and stellar masses inferred. Figure 10 shows the evolution of the stellar mass function for the whole galaxy population and

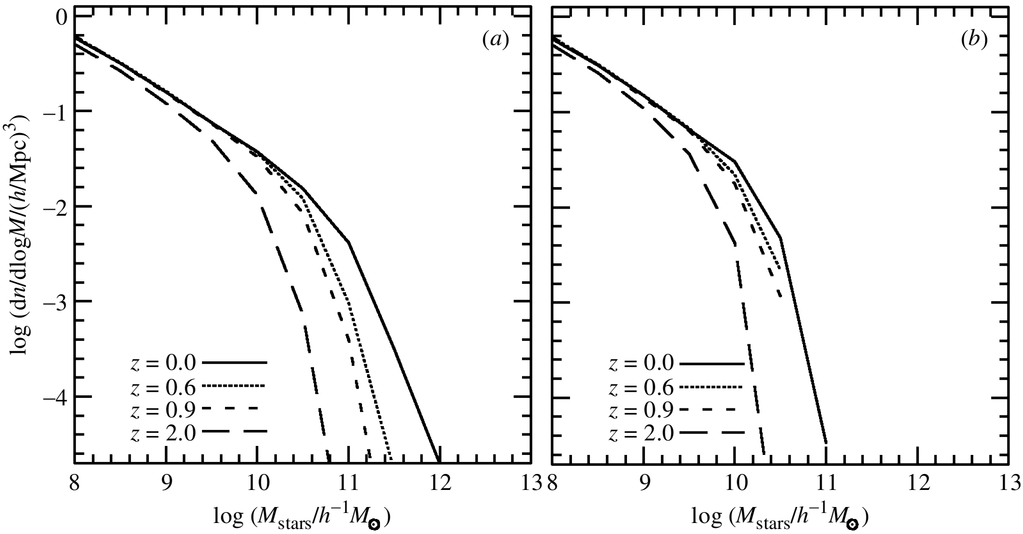

Figure 10. The evolution of the stellar mass function (a) for all galaxies and (b) for disc-dominated galaxies only.

for a subsample of disc-dominated galaxies. In both cases there is a steady monotonic evolution of the characteristic galaxy stellar mass.

(c) *Disc scale-lengths*

A prediction that is at the very heart of hierarchical galaxy formation is that galaxies were physically smaller in the past. This is quantified for our ΛCDM model by the evolving distributions of disc scale-lengths shown in figure 11.

Since the predicted distributions are broad and dependent on luminosity as well as redshift, one has to be careful to match selection criteria when comparing with observational results. This has been done in figure 12, which shows the model distribution of the scaled disc scale-length $C_{\mathrm{R}} \equiv R_{\mathrm{disc}}/M_{\mathrm{lum}}^{1/3}$ as a function of redshift for a sample chosen to match the observational sample analysed by Brinchmann (1999). The line on the plot is a fit to the observed data and indicates that the evolution detected in the scale-length distribution is broadly consistent with the expectations of this hierarchical model.

6. Conclusions

We have illustrated some of the generic features of galaxy evolution in a hierarchical model. In such models, galaxy formation is a recent process with approximately half the stars forming since redshift $z = 1.0$–1.5. The expected evolution of individual disc galaxies is complex and often involves substantial accretion and mergers. This results in there not being a one-to-one correspondence between bright galaxies at redshifts $z = 1$ and $z = 0$. The events in this complex formation history are not evident in studies of global properties such as the evolution of galaxy luminosity functions or number counts. In particular, the luminosity function evolves very little from $z = 1$ to $z = 0$. In this case, if one were to assume a one-to-one correspondence

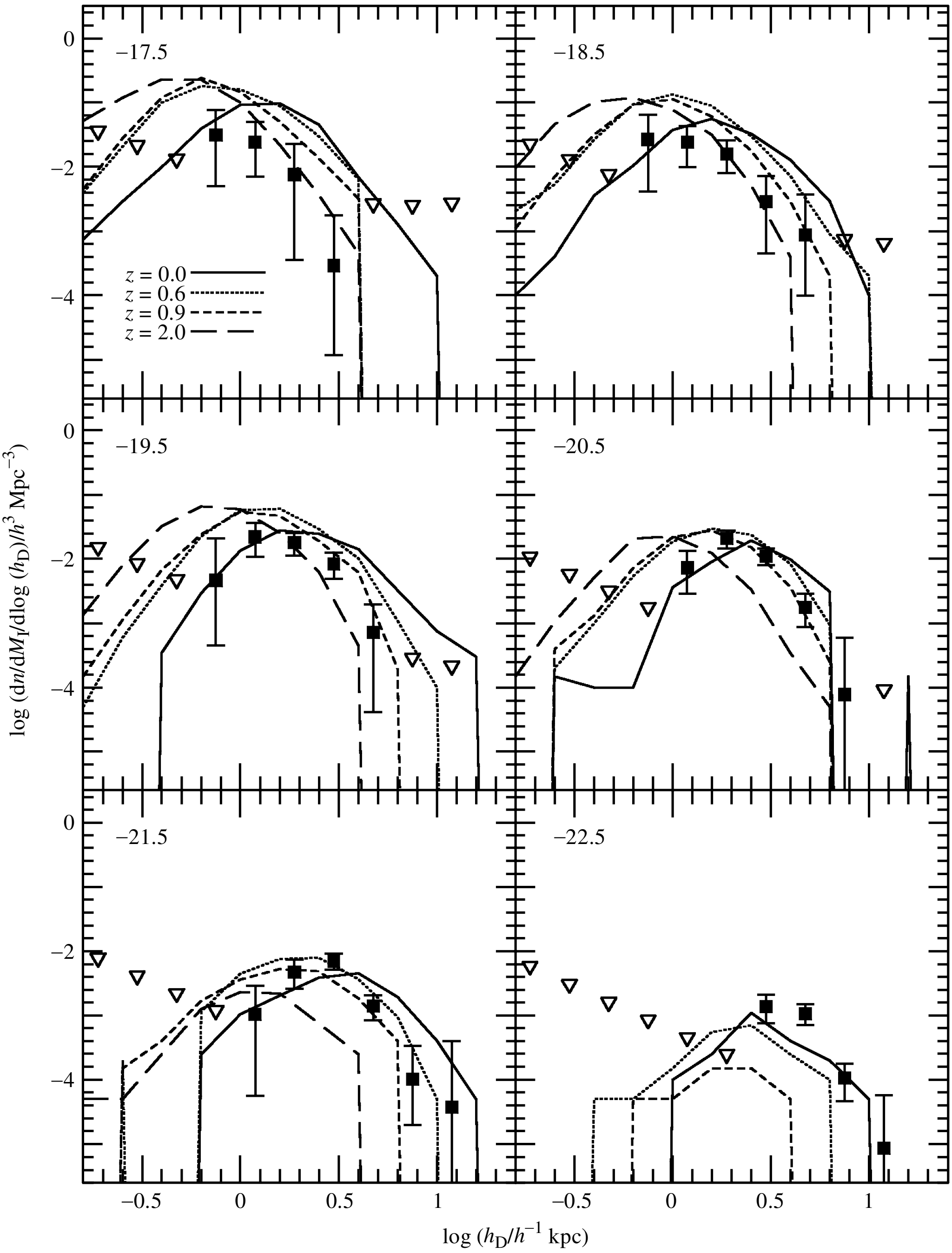

Figure 11. For different I-band absolute magnitudes the curves show the evolution of the distribution of disc scale-lengths. The data points show the observed distributions at $z = 0$ as estimated by De Jong & Lacey (2000). The triangles are their upper limits on the abundance of very large/small scale-length galaxies.

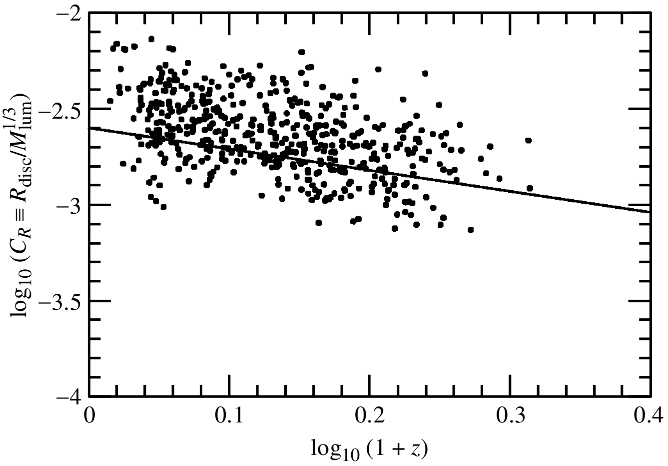

Figure 12. The points show the evolution of the scaled disc size, $C_R \equiv R_{\rm disc}/M_{\rm stars}^{1/3}$, with redshift for a sample of galaxies with $17.0 < I_{\rm AB} < 22.5$ and $R_{\rm disc} > 2h^{-1}$ kpc. The straight line is the fit found by Brinchmann (1999) for a similarly selected observational sample.

between the bright galaxies, as is done in the traditional pure luminosity evolution models (e.g. Campos & Shanks 1997), one would falsely infer that present-day disc galaxies have varied very little in luminosity since $z = 1$. The generic prediction of hierarchical galaxy formation, that the disc scale-lengths should be smaller at high redshift, has been detected and is at the level predicted by such models.

References

Abraham, R. G., Tanvir, N., Santiago, B., Ellis, R., Glazebrook, K. & van den Bergh, S. 1996 Galaxy morphology to $I = 25$ mag in the Hubble deep field. *Mon. Not. R. Astr. Soc.* **279**, L47–L52.

Adelberger, K. L., Steidel, C. C., Giavalisco, M., Dickinson, M., Pettini, M. & Kellogg, M. 1998 A counts-in-cells analysis of Lyman-break galaxies at redshift $z \sim 3$. *Astrophys. J.* **505**, 18–24.

Baugh, C. M. 1996 The real-space correlation function measured from the APM galaxy survey. *Mon. Not. R. Astr. Soc.* **280**, 267–275.

Baugh, C. M., Cole, S. & Frenk, C. S. 1996 Faint galaxy counts as a function of morphological type in a hierarchical merger model. *Mon. Not. R. Astr. Soc.* **282**, L27–L32.

Benson, A. J., Cole, S., Frenk, C. S., Baugh, C. M. & Lacey, C. G. 2000*a* The nature of galaxy bias. *Mon. Not. R. Astr. Soc.* **311**, 793.

Benson, A. J., Baugh, C. M., Cole, S., Frenk, C. S. & Lacey, C. G. 2000*b* The dependence of velocity and clustering statistics on galaxy properties. *Mon. Not. R. Astr. Soc.* (In the press.)

Brinchmann, J. 1999 The physical evolution of galaxies. PhD thesis, University of Cambridge.

Bruzual, A. G. & Charlot, S. 1993 Spectral evolution of stellar populations using isochrone synthesis. *Astrophys. J.* **405**, 538–553.

Bruzual, A. G. & Charlot, S. 2000 (In preparation.)

Campos, A. Shanks, T. 1997 Modelling the deep counts—luminosity evolution, dust and faint galaxies. *Mon. Not. R. Astr. Soc.* **291**, 383–394.

Casertano, S., Ratnatunga, K. U., Griffiths, R. E., Im, M., Neuschaffer, L. W., Ostrander, E. J. & Windhorst, R. A. 1995 Structural parameters of faint galaxies from pre-refurbishment Hubble Space Telescope medium deep survey observations. *Astrophys. J.* **453**, 599–610.

Cole, S., Lacey, C. G., Baugh, C. M. & Frenk, C. S. 2000 Hierarchical galaxy formation. *Mon. Not. R. Astr. Soc.* (Submitted.)

Dalcanton, J., Spergel, D. N. & Summers, F. 1997 The formation of disk galaxies. *Astrophys. J.* **482**, 659–676.

De Jong, R. S. & Lacey, C. G. 2000 *Astrophys. J.* (Submitted.)

Diaferio, A., Kauffmann, G., Colberg, J. M. & White, S. D. M. 1999 Clustering of galaxies in a hierarchical universe. III. Mock redshift surveys. *Mon. Not. R. Astr. Soc.* **307**, 537–552.

Driver, S. P., Windhorst, R. A., Ostrander, E. J., Keel, W. C., Griffiths, R. E. & Ratnatunga, K. U. 1995*a* The morphological mix of field galaxies to $m_{\mathrm{I}} = 24.25$ mag (b_{J} approximately 26 mag) from a deep Hubble Space Telescope WFPC2 image. *Astrophys. J.* **449**, L23–L27.

Driver, S. P., Windhorst, R. A. & Griffiths, R. E. 1995*b* The contribution of late-type/irregulars to the faint galaxy counts from Hubble Space Telescope medium-deep survey images. *Astrophys. J.* **453**, 48–64.

Ellis, R. S., Colless, M., Broadhurst, T., Heyl, J. & Glazebrook, K. 1996 Autofib redshift survey. II. Evolution of the galaxy luminosity function by spectral type. *Mon. Not. R. Astr. Soc.* **285**, 613–634.

Ferrara, A., Bianchi, S., Cimatti, A. & Giovanardi, C. 1999 An atlas of Monte Carlo models of dust extinction in galaxies for cosmological applications. *Astrophys. J. Suppl.* **123**, 437–445.

Frenk, C. S. *et al*. 1999 *Astrophys. J.* **525**, 554–582.

Gardner, J. P., Sharples, R. M., Frenk, C. S. & Carrasco, B. E. 1997 Wide-field K-band survey: the luminosity function of galaxies. *Astrophys. J.* **480**, L99–L102.

Glazebrook, K., Ellis, R., Santiago, B. & Griffiths, R. 1995*a* The morphological identification of the rapidly evolving population of faint galaxies. *Mon. Not. R. Astr. Soc.* **275**, L19–L22.

Glazebrook, K., Peacock, J. A., Miller, L. & Collins, C. A. 1995*b* An imaging K-band survey. II. The redshift survey and galaxy evolution in the infrared. *Mon. Not. R. Astr. Soc.* **275**, 169–184.

Guzzo, L. *et al*. 1999 The ESO slice project (ESP) galaxy redshift survey. VII. The redshift and real-space correlation functions. *Astron. Astrophys.* (Submitted.)

Kauffmann, G., Colberg, J. M., Diaferio, A. & White, S. D. M. 1999*a* Clustering of galaxies in a hierarchical universe. I. Methods and results at $z = 0$. *Mon. Not. R. Astr. Soc.* **303**, 188–206.

Kauffmann, G., Colberg, J. M., Diaferio, A. & White, S. D. M. 1999*b* Clustering of galaxies in a hierarchical universe. II. Evolution to high redshift. *Mon. Not. R. Astr. Soc.* **307**, 529–536.

Kennicutt, R. C. 1983 The rate of star formation in normal disk galaxies. *Astrophys. J.* **272**, 54–67.

Lacey, C. G. & Cole, S. 1993 Merger rates in hierarchical models of galaxy formation. *Mon. Not. R. Astr. Soc.* **262**, 627–649.

Lilly, S. J., Le Fevre, O., Hammer, F. & Crampton, D. 1996 The Canada–France redshift survey: the luminosity density and star formation history of the universe to z approximately 1. *Astrophys. J.* **460**, L1–L4.

Loveday, J., Peterson, B. A., Efstathiou, G. & Maddox, S. J. 1992 The Stromlo–APM redshift survey. I. The luminosity function and space density of galaxies. *Astrophys. J.* **390**, 338–344.

Mao, S., Mo, H. J. & White, S. D. M. 1998 The evolution of galactic discs. *Mon. Not. R. Astr. Soc.* **297**, L71–L75.

Marzke, R. O., da Costa, L. N., Pellegrini, P. S., Willmer, C. N. A. & Geller, M. J. 1998 The galaxy luminosity function at $z \leqslant 0.05$: dependence on morphology. *Astrophys. J.* **503**, 617–631.

Mathewson, D. S., Ford, V. L. & Buchhorn, M. 1992 A southern sky survey of the peculiar velocities of 1355 spiral galaxies. *Astrophys. J. Suppl.* **81**, 413–659.

Mo, H. J., Mao, S. & White, S. D. M. 1998 The formation of galactic discs. *Mon. Not. R. Astr. Soc.* **295**, 319–336.

Navarro, J. F. & Steinmetz, M. 1999 The cosmological origin of the Tully–Fisher relation. *Astrophys. J.* **513**, 555–560.

Navarro, J. F. & Steinmetz, M. 2000 The core density of dark matter halos: a critical challenge to the lambda-CDM paradigm? *Astrophys. J.* **528**, 607–611.

Navarro, J. F., Frenk, C. S. & White, S. D. M. 1995 The assembly of galaxies in a hierarchically clustering universe. *Mon. Not. R. Astr. Soc.* **275**, 56–66.

Navarro, J. F., Frenk, C. S. & White, S. D. M. 1997 A universal density profile from hierarchical clustering *Astrophys. J.* **490**, 493–508.

Ratcliffe, A., Shanks, T., Parker, Q. A. & Fong, R. 1998 The Durham/UKST galaxy redshift survey. II. The field galaxy luminosity function. *Mon. Not. R. Astr. Soc.* **293**, 197–207.

Steidel, C. C., Giavalisco, M., Pettini, M., Dickinson, M. & Adelberger, K. L. 1996 Spectroscopic confirmation of a population of normal star-forming galaxies at redshifts $z > 3$. *Astrophys. J.* **462**, L17–L21.

Steinmetz, M. & Navarro, J. F. 1999 The cosmological origin of disk galaxy scaling laws. In *Galaxy dynamics: from the early Universe to the present* (ed. F. Combes, G. Mamon & V. Charmandaris). Astronomical Society of the Pacific Conference Series, vol. 197, p. 165, Paris.

Zucca, E. *et al*. 1997 The ESO slice project (ESP) galaxy redshift survey. II. The luminosity function and mean galaxy density. *Astron. Astrophys.* **326**, 477–488.